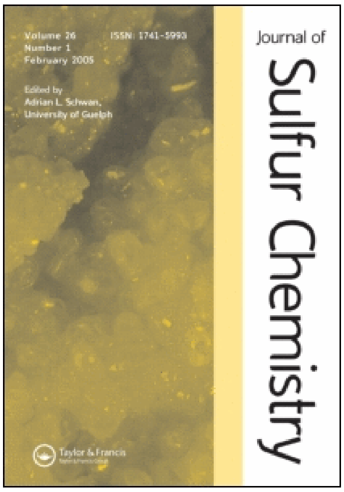

Journal of Sulfur Chemistry
Publication details, including instructions for authors and subscription information:
http://www.informaworld.com/smpp/title~content=t713926081

The synthesis of NiS, ZnS and SrS through solid-gas reaction of sulfidizing gas mixture

H. Güler[a]; F. Kurtuluş[a]
[a] Faculty of Science, Chemistry Department, Balikesir University, Balikesir, Turkey

To cite this Article Güler, H. and Kurtuluş, F.(2006) 'The synthesis of NiS, ZnS and SrS through solid-gas reaction of sulfidizing gas mixture', Journal of Sulfur Chemistry, 27: 1, 37 — 48
To link to this Article: DOI: 10.1080/17415990500505842
URL: http://dx.doi.org/10.1080/17415990500505842

Journal of Sulfur Chemistry
Vol. 27, No. 1, February 2006, 37–48

RESEARCH ARTICLE

The synthesis of NiS, ZnS and SrS through solid-gas reaction of sulfidizing gas mixture

H. GÜLER* and F. KURTULUŞ

Balikesir University, Faculty of Science, Chemistry Department, Inorganic Section, Balikesir, Turkey

(Received 7 October 2005; in final form 2 December 2005)

In this study, the sulfidizations of NiO, ZnO, $SrNO_3$ and $SrCO_3$ were investigated by using solid-gas reactions under sulfidizing gas mixture, which contains the gas mixture of carbonyl sulfide (COS), carbon disulfide (CS_2) and sulfur (S_2).

The powder crystalline forms of nickel sulfide (NiS), zinc sulfide (ZnS) and strontium sulfide (SrS) were prepared purely by solid-gas reaction technique. The product crystalline phases were characterized by the X-Ray Diffraction (XRD) technique. XRD data of the NiS, ZnS and SrS were in good agreement with the Joint Committee for Powder Diffraction Systems (JCPDS) card numbers, 2-1280, 12-688 and 8-489 in series. The crystalline grain sizes of samples were estimated by using Debye Scherrer formula. The grain sizes of the products are in the range of nano sizes.

In light of this study, it could be proposed that the compounds, NiS, ZnS and SrS could be prepared purely through sulfidizing gas mixture by solid-gas reactions under cooling of a nitrogen atmosphere.

Keywords: Sulfidizing reactions; Solid-gas synthesis; Metal sulfides; Nano sulfide materials

1. Introduction

1.1 *Metal sulfides*

More than one hundred chemical elements are known and almost all elements react with sulfur in various proportions, forming sulfides and polysulfides.

The efforts in this area are driven in part by the important technological applications found for many of these materials as well as their remarkable diversity in structure and properties.

As noted by earlier workers, the structure and bonding of most of the metal sulfides differs significantly from those of corresponding metal oxides. The differences primarily reside in the higher covalency of the metal-sulfur interactions relative to the metal-oxygen. Similarities between oxides and sulfides are most often found with the most electropositive metals [1]. For examples, the binary alkali monoxides and monosulfides both adopt the antifluorite structure type (Li_2O type). The binary monoxides and monosulfides of

---

*Corresponding author. Emails: hguler@balikesir.edu.tr; fdemiral@balikesir.edu.tr

Journal of Sulfur Chemistry
ISSN 1741-5993 print/ISSN 1741-6000 online © 2006 Taylor & Francis
http://www.tandf.co.uk/journals
DOI: 10.1080/17415990500505842

the alkaline earth metals (MN) form the rock salt structure (NaCl type). In general, the metal sulfides tend to form covalent, layered type structures in contrast to the ionic, three dimensional type structure found for the oxides. These layered materials are often highly two-dimensional with weak S....S van der Waals contacts connecting the layers (like TiS_2 and MoS_2) [2].

The lower electronegativity of the sulfur relative to the oxygen leaves the valence 3s and 3p sulfur bands much closer in energy to the transition metal d-orbital manifold (i.e., greater covalency). In many compounds, such as the copper sulfides, formal oxidation states become ambiguous and oxidation-reduction chemistry may involve the sulfide bands more than the transition metal d-orbital bands [3]. In fact, the oxidation states of the late transition metals in ternary metal sulfide complexes are still a subject of controversy.

1.2 *Electronic and conductivity properties of the metal sulfide compounds*

Just as in the case of sulfides of the main group metals, the 4s and 4p orbitals of the transition metal will combine with the 3p and 3s orbitals of sulfur to form a valence band (mainly due to sulfur) and a conduction band (mainly due to metal). These are broad bands (of the order of 10 eV) the energy gap between them is one to a few eV in most transition-metal sulfides. The 3d orbitals of the transition metal will also overlap with the sulfur orbital, but much less than the 4s and 4p orbitals of the metal. Narrow bands will be formed, but in many cases we may treat the nd orbitals as essentially localized on the metal. If this energy lies within the energy gap between the top of the valence band and the bottom of the conduction band the compound will be a semiconductor. If, however, the energy of the oxidized state also lies below/top of the valence band, the cation will be (partly) reduced, holes will be created in the valence band and the compound will be broad-band metallic conductor.

1.3 *Technological importance of nanocrystalline type of the metal sulfides, NiS, ZnS and SrS*

Metal chalcogenide nanocrystals such as NiS, ZnS, SrS, CdS and PbS have attracted great interest in recent years owing to their unique properties in physics and chemistry that significantly differ from those of their bulk counterparts. These types of material usually show novel optical, electronic and magnetic properties due to their peculiar quantum-size effect and large specific surface areas. Therefore, these metal sulfides have important applications in the field of opto-electronic technology and fabrication of photo catalysis materials [4, 5]. Nickel sulfide nanoparticles have been used as IR detectors, solar storage devices, photoconductive materials and hydrodesulfurization catalysis [6, 7]. The electromagnetic property of the nickel sulfide (NiS) is also interesting since it transforms from a paramagnetic metal to an antiferromagnetic semiconductor upon cooling under the transition temperature $T_t \sim 379\,^\circ C$ [8]. The zinc sulfide, ZnS, is an important photonic crystals and optical material with a high-refractive index and relatively low absorption in the visible spectrum [9, 10]. It is also an important semiconducting material, for other applications such as wave-guides, blue light emitting devices or a base material for the phosphors [11]. Finally, the SrS was used to obtain an efficient blue phosphor light for the full color thin film electro luminescent (TFEL) display products for many years [12].

1.4 *Thermodynamics of carbon disulfide synthesis*

Owen *et al.* [13] studied the details of the thermodynamics of carbon disulfide synthesis. A short piece of information will be given from his research.

Thermodynamic calculations are made for the following systems:

The synthesis of carbon disulfide from inorganic compounds such as hydrogen sulfide and sulfur dioxide is a problem which has long aroused interest on account of its industrial significance. In the direct reaction of hydrogen sulfide with carbon dioxide,

$$CO_2 + 2H_2S \longleftrightarrow CS_2 + 2H_2O \tag{1}$$

the equilibrium lies predominantly on the left hand side. It has been claimed, however, that the yield can be improved by adding carbon to remove the steam according to equation:

$$C + H_2O \longrightarrow CO + H_2 \tag{2}$$

and as much as 90% of the hydrogen sulfide can be converted to carbon disulfide at 950 °C in this way. Carbon disulfide may also be formed by the interaction of sulfur dioxide with carbon at high temperatures, a process on which some preliminary work, both thermodynamic and kinetic, has recently been reported by Siller [14].

Carbon disulfide can be synthesized by four different ways given below. The last one was used in our research laboratory.

$$CO_2(g) + 2H_2S(g) \tag{3}$$

$$CO_2(g) + 2H_2S(g) + \text{excess C (graphite)} \tag{4}$$

$$2H_2S(g) + \text{excess C (graphite)} \tag{5}$$

$$SO_2(g) + \text{excess C (graphite)} \tag{6}$$

All the reactions are assumed to occur at a constant total pressure of 1 atm at temperatures of 1000, 1200 and 1400 K.

A comparison of the results for systems equations 3 and 4 shows the extent to which the presence of carbon can raise the yield of carbon disulfide obtainable from hydrogen sulfide and carbon dioxide. System (equation 5) was included in order to find out if the process involving carbon dioxide offers any advantages over the reaction of carbon with hydrogen sulfide alone. The results are given in table 1.

Table 1. Percentage conversion of H_2S and SO_2.

System	Product	1000 K	1200 K	1400 K
(a) $CO_2 + 2H_2S$	CS_2	0.38	0.27	0.13
	COS	7.66	5.30	2.96
	S_2	9.55	27.12	48.68
(b) $C + CO_2 + 2H_2S$	CS_2	4.60	24.66	47.80
	COS	14.00	7.70	3.22
	S_2	0.40	2.72	6.40
(c) $C + 2H_2S$	CS_2	9.30	25.06	44.59
	S_2	0.81	2.79	5.96
(d) $C + SO_2$	CS_2	37.08	68.88	81.16
	COS	59.70	23.42	8.02
	S_2	3.22	7.70	10.82

Table 1 summarizes the equilibrium distribution of sulfur by showing the percentages of H_2S and SO_2 converted to CS_2, COS and S_2 in the four systems discussed above at 1000, 1200 and 1400 K. Table 2 contains the partial pressures of all the gases and also n, the total number of moles of gas formed. Knowledge of n is necessary when calculating percentage conversions from partial pressures. Finally, table 3 deals with the amount of heat absorbed per mole of CS_2 formed at equilibrium in systems (equations 3–6). No value is given for system (equation 3), because the yield of CS_2 is too small to be of interest.

1.5 *Discussion of the reaction involving hydrogen sulfide*

In system (equation 3), the conversion of H_2S to CS_2, which varies from 0.38% at 1000 K to 0.13% at 1400 K, appears to be negligible for industrial purposes. It is interesting to note that these percentages are much smaller than those which would have been obtained (e.g. 7.6% at 1200 K) if the formation of COS, CO and S_2 had not been taken into account. The lower figures reflect the increased partial pressure of steam formed as a result of these other reactions. As the temperature is raised, this effect is intensified by decreasing the stability of COS with respect to CO and S_2, and so the yield of CS_2 falls still further.

In the presence of carbon the conversion of H_2S to CS_2 becomes much larger; in system (equation 4) it is 4.6% at 1000 K and 47.8% at 1400 K. The decrease in the steam pressure caused by the reaction could be written as indicated before in the equation number two.

$$\mathrm{C} + \mathrm{H_2O} \longrightarrow \mathrm{CO} + \mathrm{H_2} \tag{2}$$

would, by itself, send the formation of CS_2 practically to completion, but the overall conversion is limited by the reaction;

$$\mathrm{C} + 2\mathrm{H_2}S \longrightarrow \mathrm{CS_2} + 2\mathrm{H_2} \tag{7}$$

In the latter the equilibrium lies well over on the left-hand side at 1000 K, but at 1400 K it is more even and so allows a conversion of 47.8%. A further increase of temperature would undoubtedly raise the yield still more. It should be pointed out, however, that the process represented by system (equation 4) has two important disadvantages from the industrial point of view. One is very large amount of heat absorbed, from 726 kcal at 1000 K to 111 kcal, at 1400 K, for each mole of CS_2 formed at equilibrium. The other is the high consumption of carbon.

When system (equation 4) and (equation 5) are compared, it is found that the latter is thermodynamically rather more favorable. The conversion of $2H_2S$ to CS_2, which varies from 9.3% at 1000 K to 44.6% at 1400 K, is very similar to that obtained in the presence of CO_2, but the formation of COS is avoided, only the essential amount of carbon is consumed and the overall process is much less endothermic. For industrial purposes, however about 50 kcal heat absorbed for each mole of CS_2 produced is still large.

An obvious method of avoiding the endothermicity is to add to H_2S, not CO_2, but oxygen or air. This offers the possibility of making the process thermally self-supporting without appreciably reducing the yield of CS_2 as can be seen from the following considerations. The equilibrium composition of the system:

$$2\mathrm{H_2S(g)} + \mathrm{O_2(g)} + \text{excess C (graphite)} \tag{8}$$

must be exactly the same as that of system (b), because the amount of oxygen which remains unchanged will be negligible. The overall reaction is, however, strongly exothermic.

Table 2. Equilibrium partial pressures (Atm).

	$CO_2 + 2H_2S$			$C + CO_2 + 2H_2S$			$C + 2H_2S$			$C + SO_2$		
	1000 K	1200 K	1400 K	1000 K	1200 K	1400 K	1000 K	1200 K	1400 K	1000 K	1200 K	1400 K
H_2	0.0213	0.0602	0.1167	0.0889	0.1632	0.2520	0.0969	0.2445	0.4034	–	–	–
H_2O	0.0923	0.1397	0.1800	0.01070	0.0017	0.0003	–	–	–	–	–	–
H_2S	0.5320	0.4115	0.2769	0.4250	0.3053	0.1880	0.8551	0.6334	0.3948	–	–	–
CO	0.0404	0.1056	0.1624	0.3357	0.4256	0.4250	–	–	–	0.4830	0.7303	0.7800
CO_2	0.2322	0.1669	0.1069	0.0526	0.0033	0.0003	–	–	–	0.1132	0.0087	0.0009
COS	0.0495	0.0324	0.01169	0.0736	0.0362	0.0144	–	–	–	0.3019	0.00991	0.0326
CS_2	0.0012	0.0008	0.0003	0.0120	0.0580	0.1055	0.0446	0.1100	0.1780	0.0940	0.1455	0.1646
S_2	0.0308	0.08030	0.1395	0.0010	0.0064	0.0142	0.0038	0.0123	0.0238	0.0081	0.0163	0.0220
SO_2	–	–	–	–	–	–	–	–	–	4.3×10^{-8}	8.6×10^{-9}	2.2×10^{-9}
n	3.0955	3.2712	3.4868	3.8080	4.2532	4.5374	2.1020	2.2785	2.5060	1.9775	2.3625	2.4576

Table 3. Heat absorbed per mole of CS_2 formed at equilibrium (kcal).

	1000 K	1200 K	1400 K
(a) $C + CO_2 + 2H_2S$	726	205	111
(b) $C + 2H_2S$	53	45	54
(c) $C + SO_2$	57	75	72

1.6 *The reaction of sulfur dioxide with carbon*

The yield of CS_2 is much higher in the reaction of SO_2 with carbon, i.e. 37.1% at 1000 K and 81.2% at 1400 K, than in the reaction of H_2S with carbon. At lower temperatures a considerable proportion of the SO_2 becomes COS the 59.7% so converted at 1000 K falling to 8.0% at 1400 K. From the thermal point of view, SO_2 is somewhat less favorable than H_2S, since the amount of heat absorbed per mole of CS_2 formed at equilibrium varies from 57 kcal at 1000 K to 72 kcal at 1400 K, as compared with 53 and 54 kcal for H_2S. In comparison with system (equation 4), however, system (equation 6) is more favorable in all respects.

Siller [14], in his thermodynamic analysis of the SO_2-carbon system, concluded that the maximum possible yield of CS_2 limited chiefly by the reaction:

$$C + S_2 \longrightarrow CS_2 \tag{9}$$

and is consequently about 90% throughout the temperature range considered.

Siller [14], also made an extensive series of kinetic measurements, which is of interest to compare with the present theoretical calculations. Table 4 illustrates a representative selection of his measurements with anthracite and undiluted SO_2 at atmospheric pressure. The experimental results all refer to the same rate of flow and to comparable degrees of activation of the carbon, while the temperatures are the maximum ones prevailing at the middle of the reaction zone. The equilibrium figures are obtained from those given in table 1. by graphical interpolation at the experimental temperature. It can be seen that the observed yields of CS_2 are all less than the equilibrium ones, but that those of COS are somewhat greater than the equilibrium ones; as might be expected from the increased rate of reaction, there is a closer approach to equilibrium the higher the temperature. The agreement between theory and experiment thus appears to be very satisfactory, and the observed excess of COS supports Siller's conclusion that this gas is an intermediate in the overall reaction.

The pressures of these gas mixtures are given in figure 1 and the optimum temperature was chosen between 1000 and 1100 K for our experiments.

The aim of this work is to synthesis of the metal sulfides, NiS, ZnS and SrS which have attracted great interest in recent years due to their physical and chemical properties. These metal sulfides were synthesized through the solid-gas of the sulfidizing gas mixture of COS, CS_2 and S_2.

Table 4. Percent conversions of SO_2 gases at different temperatures.

	% SO_2 converted to CS_2		% SO_2 converted to COS	
Temp. °C	Obs.	Equilib.	Obs.	Equilib.
1020	39	77	–	15
1080	48	80	14	11
1170	67	82	7	6

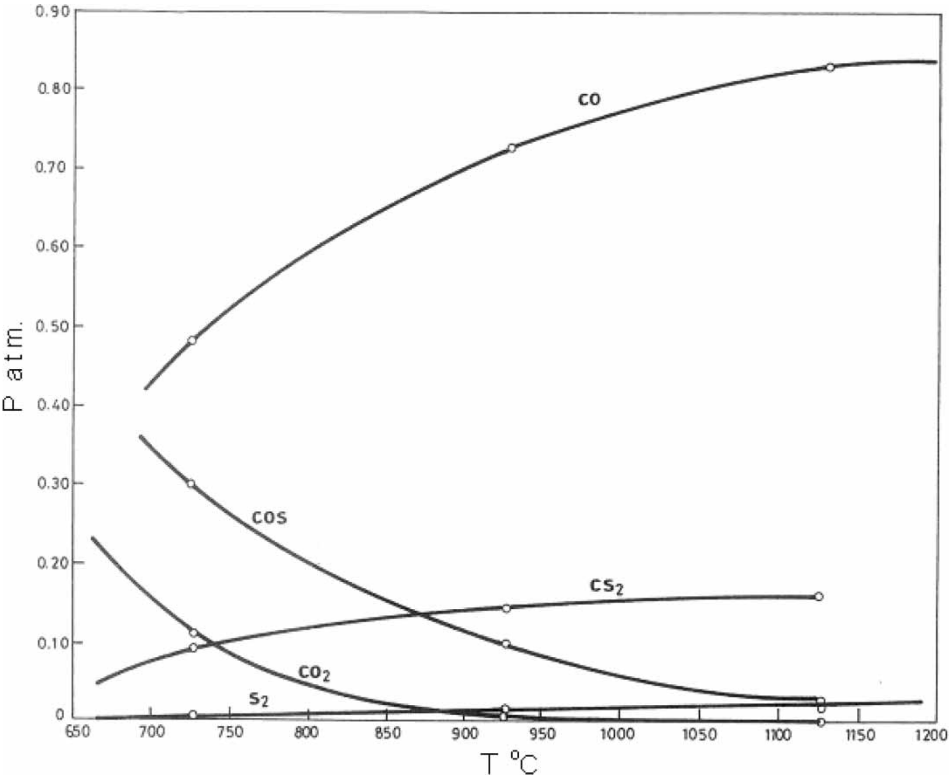

Figure 1. Plot of partial pressure vs. reaction temperature.

2. Experimental

All chemicals were of analytical grade and supplied from Merck Company. The gases were passed through $CaCl_2$ for the removal of water.

A Huber-Guiner G600 powder diffractometer which is computer controlled-automatic was used for taking X-Ray diffraction of the powders with CuK_α ($\lambda = 1.54051$ Å) radiation. 40 kV potential, and 20 mA current was used for producing X-ray radiation.

2.1 *Solid-gas reaction system*

The schematic diagram of solid-gas reaction system used in this work is given in figure 2. On the system, a horizontal tubular furnace with a silica tube of 4 cm diameter and 60 cm in length was used as reaction chamber. A vertical tube filled with activated charcoal in the furnace was used as reduction chamber. The temperature control was made with a Cr-Ni thermocouple using a temcometer type of heat control system. Polyethylene tubes with glass connections and glass valves were used in the system. In order to prevent gas leakage, a silicone type of adhesive material was employed at connections of the system.

The procedure applied in solid-gas sulfidizing reaction is as follows. The initial reactant material i.e. NiO (M = 74.71 g/mol), ZnO (M = 81.37 g/mol), $SrNO_3$ (M = 149.62 g/mol) and $SrCO_3$ (M = 147.62 g/mol) was divided to fine particles in an agate mortar by grounding. Then, this powder was put into the porcelain boat crucible of fixed weight, initially weighed, and the crucible was placed into the center of a ceramic tube in the horizontal reaction furnace.

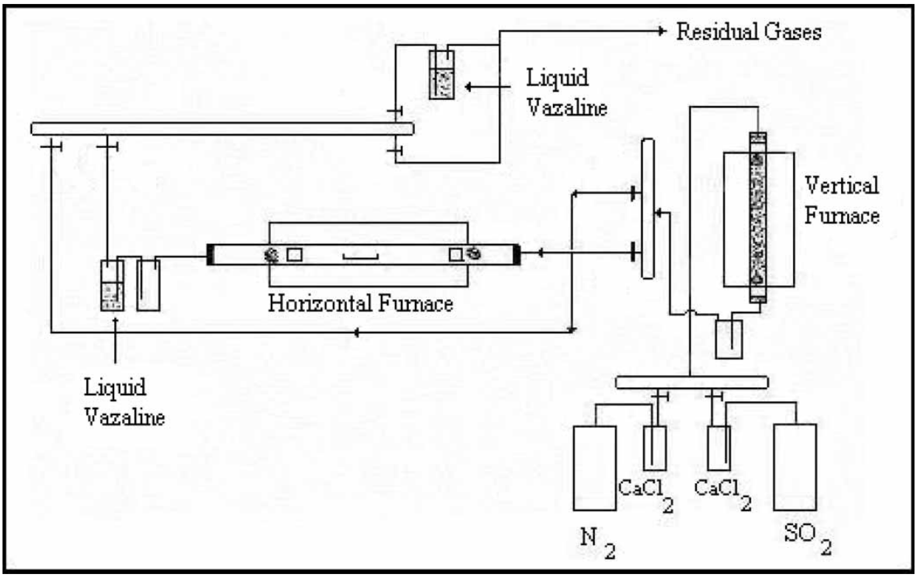

Figure 2. Flow sheet of the solid-gas system.

The ambient oxygen was removed by flowing nitrogen gas until reaching a desired reaction temperature. The gas flow rate was adjusted as such a way so that a rate of 15–20 bubbles per minute was achieved. When the system arrived at the desirable temperature, the flow of nitrogen in vertical tube furnace was adjusted to 750 °C and stopped while SO_2 gas was introduced. The optimized reaction times of 3 hours were observed. At the end of the reaction times, the SO_2 flow was terminated and a flow of nitrogen gas was initiated. The N_2 flow was continued until the system reached ambient temperature. After cooling, the closed system was opened, and the crucible was removed together with the contents from furnace. The crucible was finally weighted, and the final product was ground well in an agate mortar. In order to ensure reproducibility, the experiment was repeated three times. The phase characterization was done by XRD technique.

3. Results and discussion

3.1 *Preparation and characterization of NiS, ZnS and SrS*

On the experimental practice, the NiS, ZnS and SrS were prepared separately through solid-gas reaction of sulfidizing gas mixture of COS, CS_2, and S_2 with the initial reactants of NiO, ZnO and $SrNO_3$ (and also $SrCO_3$). Even though, the detail of the sulfidizing reactions and sulfidizing system were reported in the previous papers [15–17], we would like to give the details of the procedure and the sulfidizing reaction system for the readers of this article.

According to Welch's [18] proposal, the products in the sulfidizing gas mixture could be explained as follows:

$$SO_2(g) + 2C(s) \longrightarrow COS(g) + CO(g) \tag{10}$$

$$2COS(g) \longrightarrow CS_2(g) + CO_2(g) \tag{11}$$

$$2\mathrm{COS(g)} \longrightarrow 2\mathrm{CO(g)} + \mathrm{S_2(g)} \tag{12}$$

$$\mathrm{C(s)} + \mathrm{S_2(g)} \longrightarrow \mathrm{CS_2(g)} \tag{13}$$

When a metal oxide, MO (i.e. NiO, ZnO) or a metal nitrate (metal carbonate is also possible to use as a initial reactant) is heated in the flow of a sulfidizing gas mixture, the following reactions could take place:

$$2\mathrm{MO(s)} + \mathrm{CS_2(g)} \longrightarrow 2\mathrm{MS(s)} + \mathrm{CO_2(g)} \tag{14}$$

$$\mathrm{MO(s)} + \mathrm{COS(g)} \longrightarrow \mathrm{MS(s)} + \mathrm{CO_2(g)} \tag{15}$$

$$2\mathrm{MO(s)} + 2\mathrm{CO(g)} + \mathrm{S_2(g)} \longrightarrow 2\mathrm{MS(s)} + 2\mathrm{CO_2(g)} \tag{16}$$

When we use the $\mathrm{SrNO_3}$ as an initial reactant, the overall reaction for the synthesis of SrS could be written also as follow;

$$4\mathrm{Sr(NO_3)_2} + \mathrm{COS} + \mathrm{CS_2} + 5\mathrm{CO} + \frac{1}{2}\mathrm{S_2} \longrightarrow 4\mathrm{SrS} + 7\mathrm{CO_2} + 8\mathrm{NO_2} \tag{17}$$

But, in the case of the sulfidization of $\mathrm{SrCO_3}$, possible sulfidization reactions could be written as follows:

$$2\mathrm{SrCO_3(s)} + \mathrm{CS_2(g)} \longrightarrow 2\mathrm{SrS(s)} + 3\mathrm{CO_2(g)} \tag{18}$$

$$2\mathrm{SrCO_3(s)} + 2\mathrm{COS(g)} \longrightarrow 2\mathrm{SrS(s)} + 4\mathrm{CO_2(g)} \tag{19}$$

$$2\mathrm{SrCO_3(s)} + 2\mathrm{CO(g)} + \mathrm{S_2(g)} \longrightarrow 2\mathrm{SrS(s)} + 4\mathrm{CO_2(g)} \tag{20}$$

In this study the reactions above were adopted for the synthesis of the NiS, ZnS and SrS.

The XRD patterns of the products NiS, ZnS and SrS are given in figures 3, 4 and 5 in turn. As shown, the experimental XRD data of the NiS, ZnS and SrS were in good agreement with the JCPDS card numbers 2-1280 (crystal system was unidentified), 12-688

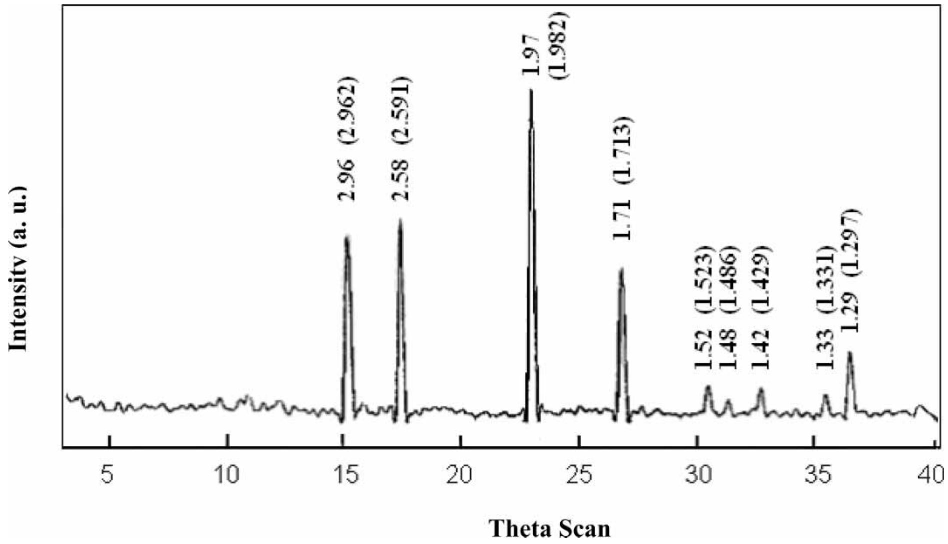

Figure 3. X-ray powder diffraction pattern of NiS synthesized at 750°C under the sulfidizing gas mixture, radiation, CuK_α (1.5405 Å) ('d' and '$\mathrm{d_{obs}}$' values were given on the figure of XRD pattern).

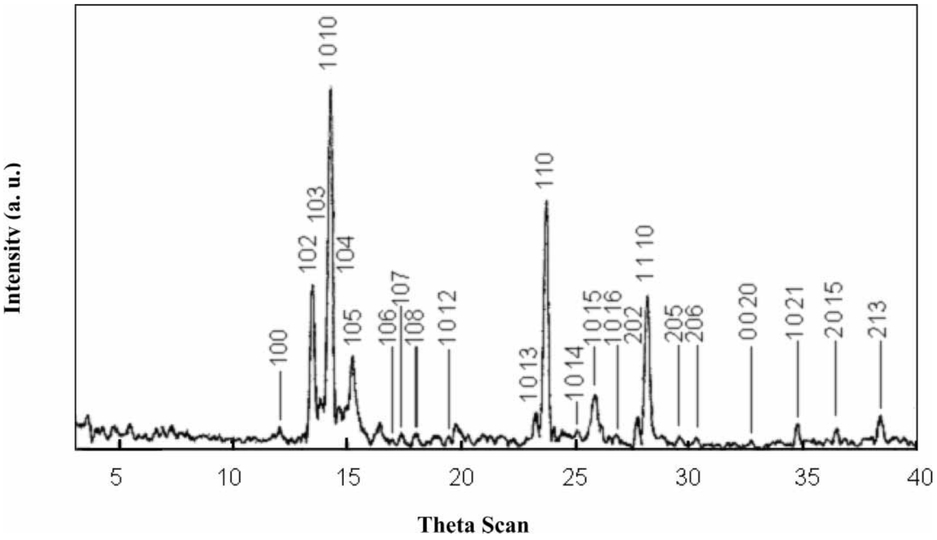

Figure 4. X-ray powder diffraction pattern of ZnS synthesized at 750°C under the sulfidizing gas mixture, radiation, CuK$_\alpha$ (1.5405 Å).

(hexagonal structure, a = 3.82, c = 31.20 Å, space group = P6$_3$mc and Z = 10) and 8-489 (cubic structure, a = 6.020 Å, space group = Fm3m and Z = 4) in a series. We obtained the same XRD patterns for the SrS compound with the sulfidization of the raw materials, SrNO$_3$ and SrCO$_3$. It could be concluded that both initial reactants could be used as an initial reactant for the synthesis of SrS. For comparison the experimental and the literature 'd' values were listed in tables 5, 6 and 7 respectively.

3.2 *Calculation of the crystalline grain size of the products, NiS, ZnS and SrS*

Calculation of the crystalline grain size of the synthesized products of the metal sulfides NiS, ZnS and SrS were done by using Debye Scherrer formula [19]. The Scherrer equation is

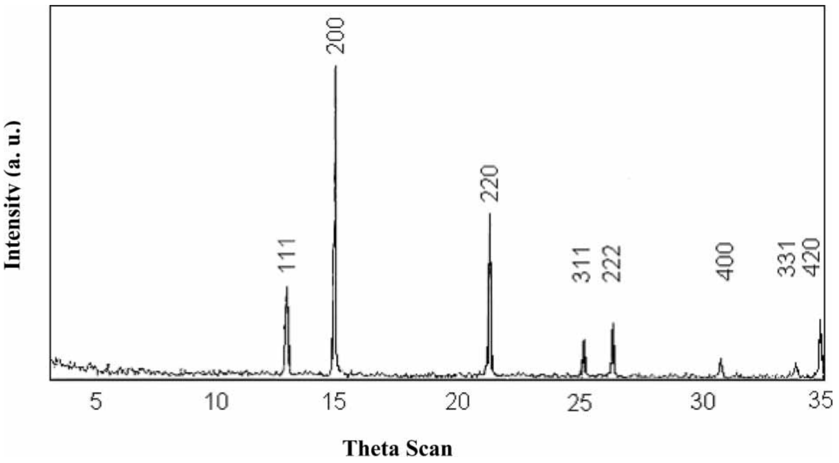

Figure 5. X-ray powder diffraction pattern of SrS synthesized at 750°C under the sulfidizing gas mixture, radiation, CuK$_\alpha$ (1.5405 Å).

Table 5. The literature and observed XRD data of NiS (JCPDS card no:2-1280).

I	d	$d_{obs.}$
80	2.96	2.9617
70	2.58	2.5911
100	1.97	1.9816
80	1.71	1.7135
30	1.52	1.5234
30	1.48	1.4863
30	1.42	1.4299
30	1.33	1.3312
60	1.29	1.2970

written as follows:

$$t = \frac{0.9\lambda}{B\cos\theta_B} \tag{21}$$

Where in the equation (21), λ is the wavelength of the X-ray radiation and B is the full width at half maximum of peak of the XRD pattern.

Scherrer demonstrated in 1918 that the size of a diffracting crystallite is directly related to the width of the X-ray diffraction peaks arising from its crystalline structure. For crystallite sizes less than about 100 nm, this size-induced peak-broadening effect may be measured accurately enough to deduce an average grain size in the sample. The XRD patterns show peaks at about $\theta = 22.90°$ (NiS), 14.28° (ZnS) and 14.99° (SrS) were due to the Bragg reflections from the Miller planes of NiS, ZnS and SrS, respectively. The grain sizes (D) of the NiS, ZnS and SrS were calculated as 25.871, 32.806 and 98.690 nm in order. The results show that the crystalline grain sizes of the NiS, ZnS and SrS have in the range of nano extension.

Table 6. The literature and observed XRD data of ZnS (JCPDS card no:12-688).

I	d	$d_{obs.}$	h	k	l	I	d	$d_{obs.}$	h	k	l
2	3.31	3.30	1	0	0	2	1.871	1.871			
6	3.26	3.26	1	0	2	2	*	1.841	1	0	14
4	3.20*	3.20				4	1.841	1.766	1	0	15
2	3.16	3.16	1	0	3	2	1.756	1.678	1	0	16
100	3.12	3.123	0	0	10	2	1.678	1.656	2	0	2
4	3.09*	3.09				35	1.649	1.630	1	1	10
4	3.05	3.04	1	0	4	2	1.626	1.598	2	0	5
6	2.93	2.93	1	0	5	2	1.598	1.572	2	0	6
2	2.81	2.81	1	0	6	2	1.572	1.558	0	0	20
2	2.76*	2.76				2	1.558	1.352	1	0	21
4	2.71	2.72				2	1.350	1.296	2	0	15
2	2.66	2.66	1	0	7	4	1.294	1.242	2	1	3
2	2.61*	2.57				2	1.239				
2	2.52	2.52	1	0	8	2					
2	2.49*	2.49				6					
2	2.08	2.28	1	0	12	2					
2	1.977*	1.977				4					
2	1.937	1.937	1	0	13	4					
50	1.904	1.912	1	1	0	6					

*Reflection which comes from the polytpe ZnS, wurtzide-8H.

Table 7. The literature and observed XRD data of SrS (JCPDS card no:8-489).

I	d	d_{obs}	h	k	l
30	3.479	3.479	1	1	1
100	3.007	3.002	2	0	0
50	2.129	2.1301	2	2	0
14	1.814	1.816	3	1	1
16	1.7378	1.739	2	2	2
12	1.5045	1.5060	4	0	0
6	1.3814	1.3810	3	3	1
14	1.3664	1.3665	4	2	0

4. Conclusion

The following conclusions could be deduced from this work:

A chemical reaction had taken place between the NiO, ZnO and $SrCO_3$ and the sulfidizing gas mixture (COS, CS_2, S_2) under cooling with inert nitrogen gas. The powder crystalline forms of NiS, ZnS and SrS were prepared purely by solid-gas reaction.

The powder crystalline phases were characterized by the XRD technique, and the XRD data of the experimental products of the NiS, ZnS and SrS were in excellent agreement with the JCPDS card numbers, 2-1280, 12-688 and 8-489 in series.

Crystalline grain sizes of the samples were calculated by using Debye Scherrer formula. The calculations showed that the crystalline grain sizes of the products are in the order of nano sizes.

In light of this study, it could be proposed that the compounds, NiS, ZnS and SrS could be prepared purely through sulfidizing gas mixture by solid-gas reaction under cooling of a nitrogen atmosphere.

Acknowledgement

The authors would like to thank the Chemistry Departments of Balikesir University and the Middle East Technical University for use of the facilities for solid-gas reaction systems.

References

[1] M. Kızılyallı, H.M. Kızılyalli. In *The Preparation of Nonstoichiometric Sulfides by Solid-Gas Reactions, Transport in Nonstoichiometric Compounds*, G. Simkovich (Ed.), p. 441, Plenum Publ. Corp. (1985).
[2] P.A. Cox. *Inorganic Chemistry*, pp. 173–174, Garland Science (UK) (2004).
[3] A. Wold. *Solid State Chemistry*, p. 203, Chapman and Hall, New York (1993).
[4] I. Honma, S. Hirakawa, K. Yamada, J.M. Bae. *Solid State Ionics*, **118**, 29 (1999).
[5] M.L. Curri, R. Comparelli, P.D. Cozzoli, G. Mascolo, A. Agostiano. *Mater. Sci. Eng., C, Biomim. Mater., Sens. Syst.*, **23**, 285 (2003).
[6] W.J.J. Welters, G. Vorbeck, H.W. Zandbergen, J.W. Dehaan, V.H.J. Vansaten, R.A. Vansaten. *J. Catal.* **150**, 155 (1994).
[7] S.D. Sartale, C.D. Lokhande. *Mater. Chem. Phys.*, **72**, 101 (2001).
[8] D.W. Bishop, P.S. Thomas, A.S. Ray. *Mater. Res. Bull.*, **33**, 1303 (1998).
[9] N.A. Dhas, A. Zaban, A. Gedanken. *Chem. Mater.*, **11**, 806 (1999).
[10] H. Zhang, F. Huang, B. Gilbert, J.F. Banfield. *J. Phys. Chem. B*, **107**, 13051 (2003).
[11] S.D. Sartale, B.R. Sankapal, M.A. Lux-Steiner Ennaoui, *Thin Solid Films*, **480–481**, 168 (2005).
[12] Sey-Shing. *Sun Displays*, **19**, 145 (1999).
[13] A.J. Owen, K.W. Sykes, D.J.D. Thomas. *Trans Faraday Soc.*, **47**, 419 (1951).
[14] C.W. Siller. *Ind. Eng. Chem.*, **40**, 1227 (1948).
[15] H. Güler, M. Kızılyallı, F. Tezer, M. Özenbaş. *High Temp. Mat. Sci.*, **38**, 23 (1997).
[16] H. Güler, B. Keşanlı, M. Kızılyallı, Ö. Pamuk, A. Morkan. *Key Eng. Mat.*, **264–268**, 33 (2004).
[17] H. Güler, M. Kızılyallı, İ. Kadan, F. Kurtuluş. *Key Eng. Mat.*, **264–268**, 1325 (2004).
[18] A.J.E. Welch. *Interim Report*, Imperial College, London (1970).
[19] B.D. Cullity, *Elements of X- ray diffraction*, 2nd Edition, Addison Wesley, Reading, MA (1978).